Partial Differential Equations and Applications (2023) 4:50
https://doi.org/10.1007/s42985-023-00267-7

ORIGINAL PAPER

Solving stationary inverse heat conduction in a thin plate

Jennifer Chepkorir[1,2] · Fredrik Berntsson[1] · Vladimir Kozlov[1]

Received: 16 January 2023 / Accepted: 16 October 2023 / Published online: 10 November 2023

Abstract
We consider a steady state heat conduction problem in a thin plate. In the application, it is used to connect two cylindrical containers and fix their relative positions. At the same time it serves to measure the temperature on the inner cylinder. We derive a two dimensional mathematical model, and use it to approximate the heat conduction in the thin plate. Since the plate has sharp edges on the sides the resulting problem is described by a degenerate elliptic equation. To find the temperature in the interior part from the exterior measurements, we formulate the problem as a Cauchy problem for stationary heat equation. We also reformulate the Cauchy problem as an operator equation, with a compact operator, and apply the Landweber iteration method to solve the equation. The case of the degenerate elliptic equation has not been previously studied in this context. For numerical computation, we consider the case where noisy data is present and analyse the convergence.

Keywords Cauchy problem · Stationary heat equation · Degenerate elliptic equation · Landweber iterative method

Mathematics Subject Classification 65N20 · 65N21 · 35D30

1 Introduction

Determination of the temperature on an inaccessible part of the boundary, by given available measurements on another part of the boundary, has many industrial applications related to engineering and science. Some of these applications are metal quenching [23], combustion [19], steel industry [34, 38], brakes [40], among many others. They are referred to as inverse heat conduction problems. This area of research have been studied extensively, in $1D$ setting, by various authors, such as [3, 4, 11, 14, 15, 21, 39]. The Cauchy problem for the steady-state anisotropic heat conduction in $2D$ and $3D$ has also been considered in [37].

The manuscript belongs to Applications of PDEs edited by Hyeonbae Kang.

✉ Jennifer Chepkorir
jennifer.chepkorir@liu.se

1 Department of Mathematics, Linköping University, 581 83 Linköping, Sweden

2 Department of Applied Mathematics, University of Nairobi, P.O. Box 30197, Nairobi, Kenya

In our research paper, we consider two cylindrical containers connected by a thin plate. This situation models a thermos bottle where a liquid is contained in the interior cylinder and the outer cylinder is a protective shell. The thin plate allows for heat conduction between the two cylinders, which allows us to monitor the temperature of the interior cylinder. The thin plate that connects the two cylinders is a $3D$ volume which is denoted by A, as shown in Fig. 1,

$$A = \{x, y, z : (x, y) \in \Omega, \quad and \quad -c(x) \leq z \leq c(x)\},$$

where

$$\Omega = (0, b) \times (0, a).$$

We assume that $c(x)$ is a differentiable and a continuous function, that behaves like a linear function near the end points $x = 0$ or $x = b$, and that $c(0) = c(b) = 0$. The space of function that contain the solution to the problem is denoted by $V(\Omega)$. More details are given in Sect. 2. The domain Ω is illustrated in Fig. 2.

The main goal of this research is to find the temperature in the interior part from the exterior measurements. We approximate the heat conduction in the thin plate by the following two dimensional steady-state heat conduction problem, with no heat generation, as follows

$$-\frac{\partial}{\partial x}\left(c(x)\frac{\partial T}{\partial x}\right) - \frac{\partial}{\partial y}\left(c(x)\frac{\partial T}{\partial y}\right) + \frac{2h}{k}\sqrt{1 + (c'(x))^2}(T - T_\infty) = 0, \tag{1.1}$$

where T is subject to the boundary conditions

$$\lim_{x \to 0, b} c(x)\frac{\partial T}{\partial x} = 0. \tag{1.2}$$

Here k is the thermal conductivity [W/m·°C], h is the convection heat transfer coefficient [W/m^2·°C], $c(x)$ is the thickness of the plate. We assume that the ambient temperature $T_\infty = 0$, because the equation is linear. The Eq. (1.1) is a degenerate elliptic equation since the coefficient $c(x)$ vanishes at $x = 0$ or $x = b$. We consider the following Cauchy problem for stationary heat equation

$$\begin{cases} -\frac{\partial}{\partial x}\left(c(x)\frac{\partial T}{\partial x}\right) - \frac{\partial}{\partial y}\left(c(x)\frac{\partial T}{\partial y}\right) + \frac{2h}{k}\sqrt{1 + (c'(x))^2}T = 0 & \text{in} \quad \Omega, \\ T = f & \text{on} \quad \Gamma_0, \\ \frac{\partial T}{\partial y} = g & \text{on} \quad \Gamma_0, \\ \lim_{x \to 0, b} c(x)\frac{\partial T}{\partial x} = 0 & \text{on} \quad \Gamma_{2,3}, \end{cases} \tag{1.3}$$

where f and g are specified temperature and net heat flux at Γ_0. Our aim is to compute both the temperature ζ and net heat flux η at Γ_1. This problem is ill-posed [20], i.e. a small perturbation in the Cauchy data results in a large error in the solution. Thus classical numerical methods cannot be used to solve such a problem. Therefore, in previous works regularization methods have been introduced to stabilize the solution. Such methods as the Tikhonov and the Fourier regularization methods [6, 13], Methods for filtering data such as Wavelet and Fourier method [16], Boundary element method [29], the Landweber iterative method [31], and the Conjugate gradient method [35] have been used to analysed such problems.

The alternating algorithm was initially proposed in [26, 27], for solving Cauchy problems for linear elliptic equations. The method consists of solving a sequence of boundary value problems. We alternate between Dirichlet and Neumann conditions on a part of the boundary. Previously, it has been developed in various directions, see [2, 9, 12, 24, 30, 32]. In

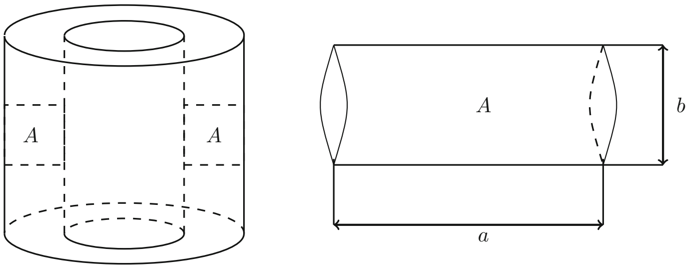

Fig. 1 The description of the engineering situation we are studying with two cylinders connected by a thin plate A. The plate is shown on the right

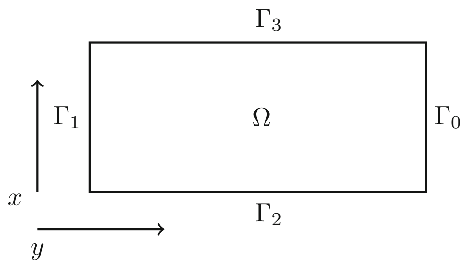

Fig. 2 Description of the two dimension domain Ω with a thickness given by $2c(x)$, whose boundary Γ is divided into four parts Γ_0, Γ_1, Γ_2 and Γ_3. Here, the solution is unknown on Γ_1, and Γ_0 is where the solution is known. The boundary data (1.2) is given on Γ_2 and Γ_3

particular [32], it was shown that the Dirichlet–Neumann algorithm is equivalent to solving Landweber iterations for an operator equation. The alternating algorithm has the advantage that they involve only boundary value problem of the same differential equation with different boundary conditions. The corresponding operator equation is also defined by solving the same differential equation with different boundary conditions. This means that we can easily solve problems with variable coefficients in domains with a complicated geometry. The regularizing properties of the algorithm are achieved by an appropriate choice of the boundary conditions [26].

In this work, we consider several methods for solving the Cauchy problem for the stationary heat equation. All of them involve the following two well-posed problems:

$$\begin{cases} -\frac{\partial}{\partial x}\left(c(x)\frac{\partial T}{\partial x}\right) - \frac{\partial}{\partial y}\left(c(x)\frac{\partial T}{\partial y}\right) + \frac{2h}{k}\sqrt{1+(c'(x))^2}T = 0 & \text{in } \Omega, \\ T = f & \text{on } \Gamma_0, \\ \frac{\partial T}{\partial y} = \eta & \text{on } \Gamma_1, \\ \lim_{x\to 0,b} c(x)\frac{\partial T}{\partial x} = 0 & \text{on } \Gamma_{2,3}, \end{cases} \tag{1.4}$$

and

$$\begin{cases} -\frac{\partial}{\partial x}\left(c(x)\frac{\partial T}{\partial x}\right) - \frac{\partial}{\partial y}\left(c(x)\frac{\partial T}{\partial y}\right) + \frac{2h}{k}\sqrt{1+(c'(x))^2}T = 0 & \text{in } \Omega, \\ \frac{\partial T}{\partial y} = g & \text{on } \Gamma_0, \\ T = \zeta & \text{on } \Gamma_1. \\ \lim_{x\to 0,b} c(x)\frac{\partial T}{\partial x} = 0 & \text{on } \Gamma_{2,3}, \end{cases} \tag{1.5}$$

where $f \in H^{1/2}(\Gamma_0)$, $\eta \in H^{-1/2}(\Gamma_1)$, $g \in H^{-1/2}(\Gamma_0)$ and $\zeta \in H^{1/2}(\Gamma_1)$. The spaces $H^{-1/2}$ and $H^{1/2}$ are trace spaces for the degenerate Sobolev spaces connected with the quadratic form associated with the operator in Ω given in (1.3). The definition of these spaces can be found in Sect. 2.2.

The first method is the Dirichlet–Neumann Alternating algorithm which can be described as follows:

(1) The first approximate temperature T_0 is obtained by solving (1.4), where η is an arbitrary initial approximation of the net heat flux on Γ_1.
(2) Having constructed T_{2j}, we find T_{2j+1} by solving (1.5) with $\zeta = T_{2j}$ on Γ_1.
(3) We then determine T_{2j+2} by solving (1.4) with $\eta = \frac{\partial T_{2j+1}}{\partial y}$ on Γ_1.

The problems (1.4) and (1.5) are well-posed as it is shown in Sect. 2.2. It is proven in Sect. 2.4, that the alternating algorithm is convergent. Since the convergence of this method is slow we consider alternative methods. The goal is to develop frame work of operator equations that can enable us to define the scalar products which helps in computation of the adjoint operator and also appropriate norms. Thus, faster convergence method can be considered.

The second method for solving the Cauchy problem (1.3) is based on rewriting the problem as an operator equation, see [4, 5, 8, 10, 32] for similar work. We introduce the operator

$$K : H^{-1/2}(\Gamma_1) \to H^{-1/2}(\Gamma_0)$$

by

$$K\eta = \partial_y T(x, 0),$$

where T is the solution of problem (1.4) with $f = 0$. Now the Cauchy problem (1.3) can be written as an operator equation, with compact operator K

$$K\eta = \xi, \tag{1.6}$$

where $\xi = g - \partial_y T(x, 0)$ and T solves problem (1.4) with $\eta = 0$. It is important to have a good description of the adjoint operator K^* for K. The operator K^* can be describe as follow

$$K^* g = \partial_y T(x, a),$$

where T is the solution to the problem (1.5) with $\zeta = 0$. The operators K and K^* are explained in more details in Sect. 3.

To solve problem (1.6), the operator K can be approximated by a matrix, and traditional methods such as Conjugate gradient method can be applied. Since K can be approximated by a matrix explicitly we can also use Tikhonov regularization method and truncated singular value decomposition (TSVD). In our previous work [5], the Landweber iteration method has been used to solve different operator equation. This method was initially proposed by Landweber in [28]. We wish to use the same method to solve the operator equation (1.6).

In this paper we analyse convergence of the Landweber iteration method, defined as: Let $\eta_0 = 0$ be the starting guess and compute

$$\eta_{m+1} = \eta_m + \alpha K^*(\xi - K\eta_m) = (I - \alpha K^* K)\eta_m + \alpha K^* \xi, \tag{1.7}$$

for $m = 0, 1, 2, \ldots$, where α is the relaxation parameter. It is well known that Landweber iterations (1.7) are convergent provided that

$$0 < \alpha < \frac{2}{||K||^2}. \tag{1.8}$$

The proof is quite similar to that for the Richardson iteration in [36, Example 4.1].

The following is an outline of the paper. In Sect. 1.1, we derive the mathematical model for the problem considered. In Sect. 2, we analyse the properties of the direct problem and show that it's well-posed. We give a proof for the convergence of the Dirichlet–Neumann alternating algorithm in Sect. 2.4. In Sect. 3, we reformulate the Cauchy problem (1.3) as an operator equation, and show that it is well-defined. We also introduce the Landweber iterations method for solving the operator equation in the same section. We discretize the differential equation (1.11) using finite difference scheme, and also, present numerical results in Sect. 4. Finally, in Sect. 5, we analyse the results, and draw some conclusion.

1.1 Derivation of the mathematical model

In this section, we derive the mathematical model of heat transfer in the thin plate, and also it's related boundary conditions.

Let us consider the two dimensional domain Ω shown in Fig. 2. Pick a small volume element of length Δy and width Δx whose thickness is $2c(x)$. To derive the mathematical model, we consider an energy balance equation on the volume element where heat flow in both $x-$ and $y-$ direction as follows;

$$Q = q_x - q_{x+\Delta x} + q_y - q_{y+\Delta y} - q_c,$$

where Q is the rate of temperature change with respect to time, q_x and q_y is obtained using Fourier's law of heat conduction and finally, q_c is the convection heat transfer given in terms of Newton's law of cooling, see [22], we obtain

$$C_p \cdot \rho \cdot c(x) \cdot \Delta x \cdot \Delta y \frac{\partial T}{\partial t} = -kA_x \frac{\partial T}{\partial x}(x, y) + kA_x \frac{\partial T}{\partial x}(x + \Delta x, y) - kA_y \frac{\partial T}{\partial y}(x, y) \tag{1.9}$$

$$+kA_y \frac{\partial T}{\partial y}(x, y + \Delta y) - 2hA_c(T - T_\infty), \tag{1.10}$$

where C_p is the specific heat capacity [J/kg·°C], ρ is the density [kg/km^3], A_x is the cross section area of the thin plate as a function of x, A_y is the cross section area of the thin plate as a function of y, and A_c is the cross section area for convective heat transfer.

Dividing both sides of (1.9) by $\Delta y \cdot \Delta x$ and taking the limits $\Delta y \to 0$ and $\Delta x \to 0$, we obtain

$$C_p \cdot \rho \cdot c(x) \frac{\partial T}{\partial t} = \frac{\partial}{\partial x}\left(kc(x)\frac{\partial T}{\partial x}\right) + \frac{\partial}{\partial y}\left(kc(x)\frac{\partial T}{\partial y}\right) - 2h\sqrt{1 + (c'(x))^2}(T - T_\infty),$$

where k is the thermal conductivity coefficient and h is the convection heat transfer coefficient.

For the steady state heat transfer, and assuming that $T_\infty = 0$, we obtain

$$\frac{\partial}{\partial x}\left(c(x)\frac{\partial T}{\partial x}\right) + \frac{\partial}{\partial y}\left(c(x)\frac{\partial T}{\partial y}\right) - \frac{2h}{k}\sqrt{1 + (c'(x))^2}T = 0. \tag{1.11}$$

Similarly, we derive the boundary conditions on Γ_2 and Γ_3, as shown in Fig. 2, and we obtain

$$\lim_{x \to 0, b} c(x)\frac{\partial T}{\partial x} = 0. \tag{1.12}$$

We note that their exist a limit at $x = 0$ and $x = b$, since $c(x)$ tend to zero at the end points. This does not necessarily mean that the limit of $\frac{\partial T}{\partial x}$, as x approaches the boundary, is zero, or even bounded.

2 Properties of the auxiliary problems

In this section, we compute solutions of (1.11) subject to the boundary condition (1.12) using the method of separation of variables. We define the bilinear form associated to the two auxiliary problems (1.4) and (1.5), and show that the weak formulation of these problems are well-posed. We also introduce two norms for each of the spaces $H^{-1/2}(\Gamma_0)$ and $H^{-1/2}(\Gamma_1)$, and show that they are equivalence. Finally, we state the theorem for the convergence of the Dirichlet–Neumann alternating algorithm.

2.1 Separation of Variables

To find solution of the differential equation (1.11) together with the boundary conditions (1.12), we will use the method of separation variables. Let

$$T(x, y) = \psi(x)\phi(y). \tag{2.13}$$

Substituting (2.13) in the differential equation (1.11) and separating variables, we get

$$\frac{1}{c(x)\psi}\partial_x(c(x)\psi_x) - \frac{2h}{c(x)k}\sqrt{1+(c'(x))^2} = -\lambda, \tag{2.14}$$

and

$$\frac{\phi_{yy}}{\phi} = \lambda, \tag{2.15}$$

where λ is a constant. Taking into account the boundary conditions (1.12) we arrive at the following spectral problem

$$\begin{cases} -\partial_x(c(x)\psi_x) + \frac{2h\psi}{k}\sqrt{1+(c'(x))^2} = \lambda c(x)\psi, \\ \lim_{x\to 0,b} c(x)\psi_x = 0. \end{cases} \tag{2.16}$$

Due to the linear behaviour of the coefficient $c(x)$ near the end points the spectrum of problem (2.16) consist of simple positive eigenvalues which are denoted by λ_j, $j = 1, 2, \ldots$, we enumerate them in the increasing order, i.e.

$$0 < \lambda_1 < \lambda_2 < \lambda_3 < \cdots .$$

The corresponding eigenfunction we denote by ψ_j and they are chosen to satisfy the bi-orthogonality conditions

$$\int_0^b c(x)\psi_j^2(x)\,dx = 1 \ \text{ for } j = 1, 2, \ldots \ \text{ and } \int_0^b c(x)\psi_i(x)\psi_j(x)\,dx = 0 \ \text{ for } i \neq j. \tag{2.17}$$

Multiplying both side of (2.16) by $\psi_j(x)$, integrating the first term by parts and then applying bi-orthogonality conditions and the boundary conditions, we obtain

$$\int_0^b c(x)(\psi_{jx})^2 dx + \int_0^b \frac{2h}{k}\sqrt{1+(c'(x))^2}\psi_j^2(x)\,dx = \lambda_j, \quad j = 1, \ldots, \tag{2.18}$$

and

$$\left\{ \int_0^b c(x)(\psi_{jx})(\psi_{ix})\,dx + \int_0^b \frac{2h}{k}\sqrt{1+(c'(x))^2}\psi_j(x)\psi_i(x)\,dx = 0, \qquad \text{if } \ i \neq j. \right. \tag{2.19}$$

Next, we solve Eq. (2.15) $\phi_{yy} - \lambda_j \phi = 0$ with boundary conditions $\phi_j(0) = M_j$ and $\phi_j(a) = N_j$. As a result we get

$$\phi_j(y) = \lambda_j^{1/4}\left(M_j \frac{\sinh\sqrt{\lambda_j}(a-y)}{\sinh\sqrt{\lambda_j}a} + N_j \frac{\sinh\sqrt{\lambda_j}y}{\sinh\sqrt{\lambda_j}a}\right). \tag{2.20}$$

It is convenient to have here the factor $\lambda_j^{1/4}$ for normalization. The general solution becomes

$$T(x, y) = \sum_{j=1}^{\infty} \phi_j(y)\psi_j(x). \tag{2.21}$$

The constants M_j and N_j will be found later by using boundary conditions for $y = 0$ and $y = a$.

2.2 Solvability of the two auxiliary problems

In this section, we introduce the bilinear form associated to the operator

$$\mathcal{L}T = -\frac{\partial}{\partial x}\left(c(x)\frac{\partial T}{\partial x}\right) - \frac{\partial}{\partial y}\left(c(x)\frac{\partial T}{\partial y}\right) + \frac{2h}{k}\sqrt{1 + (c'(x))^2}T,$$

and show that the two auxiliary problems (1.4) and (1.5) are well-posed.

In what follows, we use the Green's type identity

$$\int_\Omega \mathcal{L}T_1\, T_2\, dx\, dy = \gamma(T_1, T_2) - \int_0^b \frac{\partial T_1(x,a)}{\partial y} T_2(x,a)c(x)\, dx + \int_0^b \frac{\partial T_1(x,0)}{\partial y} T_2(x,0)c(x)\, dx,$$

where

$$\gamma(T_1, T_2) = \int_\Omega \left(c(x)\left(\frac{\partial T_1}{\partial x}\right)\left(\frac{\partial T_2}{\partial x}\right) + c(x)\left(\frac{\partial T_1}{\partial y}\right)\left(\frac{\partial T_2}{\partial y}\right) + \frac{2h}{k}\sqrt{1 + (c'(x))^2}T_1 T_2\right) dx\, dy, \tag{2.22}$$

for $T_1, T_2 \in V(\Omega)$. Our aim is to express this form in terms of the coefficients N_j and M_j.

Using the representation (2.21) and bi-orthogonality conditions (2.17)-(2.19), we obtain the following formula

$$\gamma(T, T) = \int_0^a \sum_j \lambda_j \phi_j^2(y) + \phi_{jy}^2(y)\, dy. \tag{2.23}$$

In order to evaluate the right-hand side here we start from

$$\int_0^a \sum_j \phi_j^2(y)\, dy = C_j \int_0^a M_j^2 \sinh^2\sqrt{\lambda_j}(a-y)\, dy, + 2M_jN_jC_j \int_0^a \sinh\sqrt{\lambda_j}(a-y)\sinh\sqrt{\lambda_j}y\, dy + N_j^2 C_j \int_0^a \sinh^2\sqrt{\lambda_j}y\, dy,$$

where

$$C_j = \frac{\sqrt{\lambda_j}}{\sinh^2 \sqrt{\lambda_j} a}.$$

Then we integrate each term as follows: The first term is integrated by

$$\begin{aligned}\int_0^a M_j^2 \sinh^2 \sqrt{\lambda_j}(a-y)\,dy &= \frac{1}{\sqrt{\lambda_j}} \int_0^{\sqrt{\lambda_j}a} M_j^2 \sinh^2 z\,dz,\\ &= \frac{M_j^2}{2\sqrt{\lambda_j}} \left(\frac{\sinh 2\sqrt{\lambda_j}a}{2} - \sqrt{\lambda_j}a \right).\end{aligned}$$

Similarly, we evaluate the second term

$$\begin{aligned}&2M_j N_j \int_0^a \sinh \sqrt{\lambda_j}(a-y) \sinh \sqrt{\lambda_j} y\,dy,\\ &= M_j N_j \int_0^a \left(\cosh \sqrt{\lambda_j}a - \cosh \sqrt{\lambda_j}(a-2y)\right)\,dy,\\ &= M_j N_j \left(a\cosh \sqrt{\lambda_j}a - \frac{1}{\sqrt{\lambda_j}} \sinh \sqrt{\lambda_j}a \right).\end{aligned}$$

Finally, we integrate the last term

$$\int_0^a N_j^2 \sinh^2 \sqrt{\lambda_j} y\,dy = \frac{1}{\sqrt{\lambda_j}} \int_0^{\sqrt{\lambda_j}a} N_j^2 \sinh^2 z\,dz, \tag{2.24}$$

$$= \frac{N_j^2}{2\sqrt{\lambda_j}} \left(\frac{\sinh 2\sqrt{\lambda_j}a}{2} - \sqrt{\lambda_j}a \right). \tag{2.25}$$

Combining these formulas, we obtain

$$\int_0^a \phi_j^2(y)\,dy = \frac{C_j}{2\sqrt{\lambda_j}} F(\sqrt{\lambda_j}a, N_j, M_j), \tag{2.26}$$

where

$$\begin{aligned}F(z, X, Y) &= A(z)(X^2+Y^2) + 2B(z)XY, \quad A(z) = \frac{\sinh 2z}{2} - z,\\ B(z) &= z\cosh z - \sinh z.\end{aligned}$$

By (2.26) the function $F(z, X, Y)$ is positive for $z > 0$ and $X^2 + Y^2 > 0$. One can verify the inequalities

$$0 < z\cosh z - \sinh z < \frac{\sinh 2z}{2} - z \quad \text{for } z > 0.$$

This implies the existence of $\alpha_1, \alpha_2 > 0$ for each $\beta > 0$ such that

$$\alpha_2 e^{2z} \geq \frac{\sinh 2z}{2} - z - (z\cosh z - \sinh z) \geq \alpha_1 e^{2z} \quad \text{for } z \geq \beta.$$

Using the inequality

$$(A - |B|)(X^2+Y^2) \leq A(X^2+Y^2) + 2BXY \leq (A+|B|)(X^2+Y^2) \quad \text{for } A \geq |B|, \tag{2.27}$$

we obtain

$$c_1\lambda_j\left(M_j^2+N_j^2\right) \le \int_0^a \lambda_j\phi_j^2(y)\,dy \le c_2\lambda_j\left(M_j^2+N_j^2\right), \tag{2.28}$$

where the constant c_1 and c_2 are positive constants, and are independent of M_j and N_j.

Let us evaluate the second term in (2.23). We have

$$\begin{aligned}\int_0^a \sum_j(\phi_{jy})^2(y)\,dy = \lambda_j C_j \int_0^a M_j^2\cosh^2\sqrt{\lambda_j}(a-y)\,dy \\ -2M_jN_j\lambda_jC_j\int_0^a \cosh\sqrt{\lambda_j}(a-y)\cosh\sqrt{\lambda_j}y \\ +N_j^2\lambda_jC_j\int_0^a\cosh^2\sqrt{\lambda_j}y\,dy\end{aligned}$$

We integrate each term as follows: We treat the first term by

$$\begin{aligned}\int_0^a M_j^2\cosh^2\sqrt{\lambda_j}(a-y)\,dy &= \frac{1}{\sqrt{\lambda_j}}\int_0^{\sqrt{\lambda_j}a} M_j^2\cosh^2 z\,dz,\\ &= \frac{M_j^2}{2\sqrt{\lambda_j}}\left(\frac{\sinh 2\sqrt{\lambda_j}a}{2}+\sqrt{\lambda_j}a\right).\end{aligned}$$

Similarly, the second term is evaluated as

$$\begin{aligned}&-2M_jN_j\int_0^a\cosh\sqrt{\lambda_j}(a-y)\cosh\sqrt{\lambda_j}y\,dy\\ &= -M_jN_j\int_0^a\left(\cosh\sqrt{\lambda_j}a+\cosh\sqrt{\lambda_j}(a-2y)\right)dy,\\ &= -M_jN_j\left(a\cosh\sqrt{\lambda_j}a+\frac{1}{\sqrt{\lambda_j}}\sinh\sqrt{\lambda_j}a\right).\end{aligned}$$

Finally, the last term has the form

$$\int_0^a N_j^2\cosh^2\sqrt{\lambda_j}y\,dy = \frac{1}{\sqrt{\lambda_j}}\int_0^{\sqrt{\lambda_j}a}N_j^2\cosh^2 z\,dz, \tag{2.29}$$

$$= \frac{N_j^2}{2\sqrt{\lambda_j}}\left(\frac{\sinh 2\sqrt{\lambda_j}a}{2}+\sqrt{\lambda_j}a\right). \tag{2.30}$$

Combining the above formulas, we obtain

$$\int_0^a(\phi_{jy})^2(y)\,dy = \frac{C_j\lambda_j}{2}G(\sqrt{\lambda_j}a, N_j, M_j), \tag{2.31}$$

where

$$\begin{aligned}G(z,X,Y) &= A_2(z)(X^2+Y^2)-2B_2(z)XY, \quad A_2(z)=\frac{\sinh 2z}{2}+z,\\ B_2(z) &= z\cosh z+\sinh z.\end{aligned}$$

Since the function $G(z,X,Y)$ is positive, for $z>0$ and $X^2+Y^2>0$, we have

$$\frac{1}{2}G(1,1) = A_2(z)-B_2(z)>0 \ \text{ for } z>0.$$

Now using (2.27), and the positivity of $B(z)$ for $z > 0$, we get

$$C_1\lambda_j(N_j^2+M_j^2) \le \int_0^a (\phi_{jy})^2(y)\,dy \le C_2\lambda_j(N_j^2+M_j^2) \tag{2.32}$$

for some positive constants C_1 and C_2.

Combining (2.28) and (2.32), we obtain

$$C_1\sum_{j=1}^{\infty}\lambda_j(N_j^2+M_j^2) \le \gamma(T,T) \le C_2\sum_{j=1}^{\infty}\lambda_j(N_j^2+M_j^2). \tag{2.33}$$

Let us introduce the spaces of functions in Ω. The space $V(\Omega)$ consists of functions defined on Ω having a representation given by (2.21), where ϕ_j are defined by (2.20). We supply this space with the norm

$$||T||_{V(\Omega)} = \left(\sum_{j=1}^{\infty}\lambda_j(N_j^2+M_j^2)\right)^{1/2}. \tag{2.34}$$

Let also $H^{1/2}(0,b)$ be the space of functions

$$f = \sum_j f_j\psi_j(x), \quad \zeta = \sum_j \zeta_j\psi_j(x), \tag{2.35}$$

with the norms

$$||f||_{H^{1/2}(0,b)} = \left(\sum_{j=1}^{\infty}\sqrt{\lambda_j}f_j^2\right)^{1/2}, \quad ||\zeta||_{H^{1/2}(0,b)} = \left(\sum_{j=1}^{\infty}\sqrt{\lambda_j}\zeta_j^2\right)^{1/2},$$

and $H^{-1/2}(0,b)$ be the space of functions

$$\eta = \sum_j \eta_j\psi_j(x), \quad g = \sum_j g_j\psi_j(x), \tag{2.36}$$

with the norms

$$||\eta||_{H^{-1/2}(0,b)} = \left(\sum_{j=1}^{\infty}\lambda_j^{-1/2}\eta_j^2\right)^{1/2}, \quad ||g||_{H^{-1/2}(0,b)} = \left(\sum_{j=1}^{\infty}\lambda_j^{-1/2}g_j^2\right)^{1/2}. \tag{2.37}$$

If $T \in V(\Omega)$, then

$$T(x,0) = \sum_{j=1}^{\infty}\lambda_j^{1/4}M_j\psi_j(x),$$

and

$$T(x,a) = \sum_{j=1}^{\infty}\lambda_j^{1/4}N_j\psi_j(x),$$

and hence both $T(x,0)$ and $T(x,a)$ belong to $H^{1/2}(\Gamma_0)$ and $H^{1/2}(\Gamma_1)$. In order to emphasis the fact that we are dealing with the trace of function from $V(\Omega)$ on Γ_0 (Γ_1), we shall use the notation $H^{1/2}(\Gamma_0)$ and $H^{1/2}(\Gamma_1)$ instead of $H^{1/2}(0,b)$.

Furthermore,

$$\partial_y T(x,0) = \sum_{j=1}^{\infty} \lambda_j^{3/4} \left(-M_j \frac{\cosh\sqrt{\lambda_j} a}{\sinh\sqrt{\lambda_j} a} + N_j \frac{1}{\sinh\sqrt{\lambda_j} a} \right) \psi_j(x),$$

and

$$\begin{aligned} ||\partial_y T(x,0)||^2_{H^{-1/2}(0,b)} &= \sum_{j=1}^{\infty} \lambda_j \left(-M_j \frac{\cosh\sqrt{\lambda_j} a}{\sinh\sqrt{\lambda_j} a} + N_j \frac{1}{\sinh\sqrt{\lambda_j} a} \right)^2, \\ &\le C \sum_{j=1}^{\infty} \lambda_j (M_j^2 + N_j^2) = ||T||_{V(\Omega)}. \end{aligned}$$

Similarly,

$$\partial_y T(x,a) = \sum_{j=1}^{\infty} \lambda_j^{3/4} \left(-M_j \frac{1}{\sinh\sqrt{\lambda_j} a} + N_j \frac{\cosh\sqrt{\lambda_j} a}{\sinh\sqrt{\lambda_j} a} \right) \psi_j(x),$$

and

$$||\partial_y T(x,a)||^2_{H^{-1/2}(0,b)} = \sum_{j=1}^{\infty} \lambda_j \left(-M_j \frac{1}{\sinh\sqrt{\lambda_j} a} + N_j \frac{\cosh\sqrt{\lambda_j} a}{\sinh\sqrt{\lambda_j} a} \right)^2, \tag{2.38}$$

$$\le C \sum_{j=1}^{\infty} \lambda_j (M_j^2 + N_j^2) = ||T||_{V(\Omega)}. \tag{2.39}$$

To give a clear notation for the dual spaces on Γ_0 (Γ_1), we shall use $H^{-1/2}(\Gamma_0)$ and $H^{-1/2}(\Gamma_1)$ instead of $H^{-1/2}(0,b)$. More detail information about function spaces can be found in [33].

The following lemma shows that the problem (1.4) is well-posed.

Lemma 2.1 *Let $f \in H^{1/2}(\Gamma_0)$ and $\eta \in H^{-1/2}(\Gamma_1)$. Then the problem (1.4) has a unique solution $T \in V(\Omega)$ satisfying the estimate*

$$||T||_{V(\Omega)} \le C(||f||_{H^{1/2}(\Gamma_0)} + ||\eta||_{H^{-1/2}(\Gamma_1)}). \tag{2.40}$$

Proof Let

$$f(x) = \sum_{j=1}^{\infty} f_j \psi_j(x), \quad ||f||^2_{H^{1/2}(\Gamma_0)} = \sum_{j=1}^{\infty} \lambda_j^{1/2} f_j^2,$$

and

$$\eta(x) = \sum_{j=1}^{\infty} \eta_j \psi_j(x), \quad ||\eta||^2_{H^{-1/2}(\Gamma_1)} = \sum_{j=1}^{\infty} \lambda_j^{-1/2} \eta_j^2.$$

From (2.21) and the second equation in (1.4), we get

$$M_j \lambda_j^{1/4} = f_j, \quad \text{or} \quad \lambda_j M_j^2 = \lambda_j^{1/2} f_j^2. \tag{2.41}$$

Similarly using the third relation in (1.4), we obtain

$$\lambda_j^{3/4} \left(-M_j \frac{1}{\sinh\sqrt{\lambda_j} a} + N_j \frac{\cosh\sqrt{\lambda_j} a}{\sinh\sqrt{\lambda_j} a} \right) = \eta_j. \tag{2.42}$$

Multiplying both side in (2.42) with $\lambda_j^{-1/4}$ and rearranging the equation, we obtain

$$\lambda_j^{1/2} N_j \coth \sqrt{\lambda_j} a = \eta_j \lambda_j^{-1/4} + \frac{\lambda_j^{1/2}}{\sinh \sqrt{\lambda_j} a} M_j. \tag{2.43}$$

This leads to

$$\lambda_j N_j^2 \leq C(\lambda_j^{-1/2} \eta_j^2 + \lambda_j M_j^2), \tag{2.44}$$

where the constant C depends only on $\sqrt{\lambda_1} a$. Now (2.34) together with (2.41) and (2.44) implies (2.40). □

The auxiliary problem (1.5) can be analysed similarly. The corresponding solvability results is the following.

Lemma 2.2 *Let $g \in H^{-1/2}(\Gamma_0)$ and $\zeta \in H^{1/2}(\Gamma_1)$. Then the problem (1.5) has a unique solution $T \in V(\Omega)$ satisfying the estimate*

$$||T||_{V(\Omega)} \leq C(||\zeta||_{H^{1/2}(\Gamma_1)} + ||g||_{H^{-1/2}(\Gamma_0)}). \tag{2.45}$$

2.3 Equivalence of norms

In [1, 5], we use different norms for the trace functions on Γ_0 and Γ_1. These norms are more suitable for the case when we can not write the solutions explicitly, by using separation of variables. These norms are defined by using only the bilinear form $\gamma(T_1, T_2)$ given in (2.22). Their definitions can be easily extended to more general degenerate elliptic operators and domains.

Let us introduce this norms and their corresponding inner products.

Definition 2.3 Let $\eta_1, \eta_2 \in H^{-1/2}(\Gamma_1)$, and $T_1, T_2 \in V(\Omega)$ be the solution of problem (1.4) where $\eta_1 = \eta$ and $\eta_2 = \eta$ on Γ_1, and $f = 0$ on Γ_0. An inner product on the space $H^{-1/2}(\Gamma_1)$ is define as

$$\langle \eta_1, \eta_2 \rangle_1 = \gamma(T_1, T_2). \tag{2.46}$$

The corresponding norm is given by $\|\eta\|_{\gamma,\Gamma_1} = \langle \eta, \eta \rangle_1^{1/2}$.

Similarly, we can introduce the inner product for g on Γ_0 in terms of the solution of the well-posed problem (1.5).

Definition 2.4 Let $g_1, g_2 \in H^{-1/2}(\Gamma_0)$, and $T_1, T_2 \in V(\Omega)$ be the solution of problem (1.5). Here, $g_1 = g$ and $g_2 = g$ on Γ_0, and $\zeta = 0$ on Γ_1. One can define an inner product on the space $H^{-1/2}(\Gamma_0)$ as follows;

$$\langle g_1, g_2 \rangle_0 = \gamma(T_1, T_2), \tag{2.47}$$

and the corresponding norm is given by $\|g\|_{\gamma,\Gamma_0} = \langle g, g \rangle_0^{1/2}$.

Let us prove the following formulas for the inner products $\langle \cdot, \cdot \rangle_1$ and $\langle \cdot, \cdot \rangle_0$.

Lemma 2.5 *The following relations hold*

$$\langle \eta_1, \eta_2 \rangle_1 = \sum_{j=1}^{\infty} \lambda_j^{-1/2} \eta_{1j} \eta_{2j} \frac{\sinh \sqrt{\lambda_j} a}{\cosh \sqrt{\lambda_j} a}, \tag{2.48}$$

and

$$\langle g_1, g_2 \rangle_0 = \sum_{j=1}^{\infty} \lambda_j^{-1/2} g_{1j} g_{2j} \frac{\sinh \sqrt{\lambda_j} a}{\cosh \sqrt{\lambda_j} a}. \tag{2.49}$$

Proof Applying Green's type identity, we have

$$\gamma(T_1, T_2) = \int_0^b \eta_1 T_2(x, a)\, c(x)dx = \int_0^b \eta_2 T_1(x, a)\, c(x)dx. \tag{2.50}$$

Let $T_1 \in V(\Omega)$ be a solution to problem (1.4) with $f = 0$ on Γ_0. Using the representation (2.21) the solution of $T_1(x, y)$ is given by

$$T_1(x, y) = \sum_{j=1}^{\infty} \lambda_j^{1/4} N_j \frac{\sinh \sqrt{\lambda_j} y}{\sinh \sqrt{\lambda_j} a}\, \psi_j(x), \tag{2.51}$$

where $M_j = 0$ at $y = 0$ on Γ_0. Computing the derivative of (2.51) with respect to y at $y = a$, we obtain

$$\partial_y T_1(x, a) = \sum_{j=1}^{\infty} \lambda_j^{3/4} N_j \frac{\cosh \sqrt{\lambda_j} a}{\sinh \sqrt{\lambda_j} a}\, \psi_j(x). \tag{2.52}$$

The solution obtain in (2.52) is equals to

$$\eta_1(x) = \sum_{j=1}^{\infty} \eta_{1j} \psi_j(x). \tag{2.53}$$

Equating (2.52) into (2.53), and identifying the coefficient gives,

$$N_j = \eta_{1j} \lambda_j^{-3/4} \frac{\sinh \sqrt{\lambda_j} a}{\cosh \sqrt{\lambda_j} a}. \tag{2.54}$$

Substituting (2.54) in (2.51), we get

$$T_1(x, y) = \sum_{j=1}^{\infty} \lambda_j^{-1/2} \eta_{1j} \frac{\sinh \sqrt{\lambda_j} y}{\cosh \sqrt{\lambda_j} a}\, \psi_j(x). \tag{2.55}$$

The solution of $T_1(x, y)$ at $y = a$ is given by

$$T_1(x, a) = \sum_{j=1}^{\infty} \lambda_j^{-1/2} \eta_{1j} \frac{\sinh \sqrt{\lambda_j} a}{\cosh \sqrt{\lambda_j} a}\, \psi_j(x). \tag{2.56}$$

Substituting (2.56) in (2.50), and using the fact that

$$\eta_2(x) = \sum_{j=1}^{\infty} \eta_{2j} \psi_j(x),$$

we have

$$\gamma(T_1, T_2) = \int_0^b \left\{ \sum_{j=1}^{\infty} \eta_{2j} \psi_j(x) \right\} \left\{ \sum_{k=1}^{\infty} \lambda_k^{-1/2} \eta_{1k} \frac{\sinh \sqrt{\lambda_k} a}{\cosh \sqrt{\lambda_k} a}\, \psi_k(x) \right\} c(x)dx. \tag{2.57}$$

By applying bi-orthogonality conditions (2.17) in (2.57), we obtain

$$\gamma(T_1, T_2) = \sum_{j=1}^{\infty} \lambda_j^{-1/2} \eta_{2j} \eta_{1j} \frac{\sinh \sqrt{\lambda_j} a}{\cosh \sqrt{\lambda_j} a}. \tag{2.58}$$

This proves the first formula in Lemma 2.5. The second formula can be proven similarly. □

Let us now state and proof the equivalence of the norms.

Proposition 2.6 *The norm $\|\eta\|_{H^{-1/2}(\Gamma_1)}$is equivalent to the norm $||\eta||_{\gamma,\Gamma_1}$ in the space $H^{-1/2}(\Gamma_1)$ and the norm $\|g\|_{H^{-1/2}(\Gamma_0)}$ is equivalent to the norms $\|g\|_{\gamma,\Gamma_0}$in the space $H^{-1/2}(\Gamma_0)$.*

Proof Comparing (2.58) and (2.37), we see that the norms $||\eta||_{H^{-1/2}(\Gamma_1)}$ and $||\eta||_{\gamma,\Gamma_1}$ are equivalent. Similarly, comparing the second formula in Lemma 2.5 and (2.37) we also see that the norms $||g||_{H^{-1/2}(\Gamma_0)}$ and $||g||_{\gamma,\Gamma_0}$ are equivalent. □

2.4 The convergence of the Dirichlet-Neumann alternating algorithm

We now state the theorem of convergence of the Dirichlet–Neumann algorithm for solving the Cauchy problem (1.3) with the exact data, described in Sect. 1. Let $\{T_j\}_{j=0}^{\infty}$ be the iteration describe in the Dirichlet–Neumann algorithm shown in the introduction. This iterations depends on f, g and η.

Theorem 2.7 *Let $f \in H^{1/2}(\Gamma_0)$ and $g \in H^{-1/2}(\Gamma_0)$. Let also, $T \in V(\Omega)$ be the solution to problem (1.3). Then for $\eta \in H^{-1/2}(\Gamma_1)$, the sequences $\{T_j\}_{j=0}^{\infty}$ obtained using the algorithm described in Sect. 1, converges to T in $V(\Omega)$.*

Proof The proof of this theorem is similar to that in [1, 9] and therefore we do not present it here. □

3 The operator equation

In this section, we define the operator equations that are used in the numerical computations.

Definition 3.1 Let $\eta \in H^{-1/2}(\Gamma_1)$. We define the operator

$$K : \ H^{-1/2}(\Gamma_1) \to H^{-1/2}(\Gamma_0)$$

by

$$K\eta = \partial_y T_{(0,\eta)}(x, 0),$$

where $T_{(f,\eta)}$ is the solution of problem (1.4). We introduce the notation $T_{(f,\eta)}$ so that we can refer to solutions of the problem (1.4) with different boundary conditions f, η, e.g. $T_{(0,\eta)}$ solves (1.4) with $f = 0$.

Let us express the operator K in terms of the basis function $\psi_j(x)$. From (2.55), we have

$$T_{(0,\eta)}(x, y) = \sum_{j=1}^{\infty} \lambda_j^{-1/2} \eta_j \frac{\sinh \sqrt{\lambda_j} y}{\cosh \sqrt{\lambda_j} a} \psi_j(x). \tag{3.59}$$

Computing the derivative of (3.59) with respect to y at $y = 0$, we obtain

$$K\eta = \sum_{j=1}^{\infty} \eta_j \frac{1}{\cosh \sqrt{\lambda_j} a} \psi_j(x). \tag{3.60}$$

The Cauchy problem (1.3) can be written in terms of an operator equation with respect to η as follows

$$K\eta = g - \partial_y T_{(f,0)}(x,0). \tag{3.61}$$

Lemma 3.2 *Let K be given as in Definition 3.1. The expression (3.61) can be written as follows*

$$K\eta = g - \sum_{j=1}^{\infty} \lambda_j^{1/2} f_j \left(\frac{-\cosh\sqrt{\lambda_j}a}{\sinh\sqrt{\lambda_j}a} + \frac{1}{\cosh\sqrt{\lambda_j}a \sinh\sqrt{\lambda_j}a} \right) \psi_j(x). \tag{3.62}$$

Proof Using the general solution (2.21), we obtain

$$T_{(f,0)}(x,y) = \sum_{j=1}^{\infty} \lambda_j^{1/4} N_j \left(\frac{\cosh\sqrt{\lambda_j}a \sinh\sqrt{\lambda_j}(a-y)}{\sinh\sqrt{\lambda_j}a} + \frac{\sinh\sqrt{\lambda_j}y}{\sinh\sqrt{\lambda_j}a} \right) \psi_j(x), \tag{3.63}$$

where $M_j = N_j \cosh\sqrt{\lambda_j}a$ at $y = a$. From (3.63), we compute

$$f(x) = \sum_{j=1}^{\infty} f_j \psi_j(x)$$

at $y = 0$, and we obtain

$$T_{(f,0)}(x,0) = \sum_{j=1}^{\infty} \lambda_j^{1/4} N_j \cosh\sqrt{\lambda_j}a\, \psi_j(x).$$

As a result we get,

$$f_j = \sum_{j=1}^{\infty} \lambda_j^{1/4} N_j \cosh\sqrt{\lambda_j}a. \tag{3.64}$$

From (3.64) we obtain the coefficient N_j as follows

$$N_j = \frac{f_j \lambda_j^{-1/4}}{\cosh\sqrt{\lambda_j}a}. \tag{3.65}$$

Substituting (3.65) in (3.63), we obtain

$$T_{(f,0)}(x,y) = \sum_{j=1}^{\infty} f_j \left(\frac{\sinh\sqrt{\lambda_j}(a-y)}{\sinh\sqrt{\lambda_j}a} + \frac{\sinh\sqrt{\lambda_j}y}{\cosh\sqrt{\lambda_j}a \sinh\sqrt{\lambda_j}a} \right) \psi_j(x). \tag{3.66}$$

Evaluating the derivative of (3.66) with respect to y at $y = 0$, we obtain

$$\partial_y T_{(f,0)}(x,0) = \sum_{j=1}^{\infty} \lambda_j^{1/2} f_j \left(\frac{-\cosh\sqrt{\lambda_j}a}{\sinh\sqrt{\lambda_j}a} + \frac{1}{\cosh\sqrt{\lambda_j}a \sinh\sqrt{\lambda_j}a} \right) \psi_j(x). \tag{3.67}$$

Substituting (3.67) on the second term of the right-hand side in (3.61), we get the results. □

For more detail information on how to write a Cauchy problem as an operator equation, one can see for instance [5, 17].

Let us now state and proof the lemma for the adjoint operator K^*.

Lemma 3.3 *Let K be defined as in Definition 3.1, the adjoint operator*

$$K^*: \; H^{-1/2}(\Gamma_0) \to H^{-1/2}(\Gamma_1),$$

where we use the inner products $\langle\cdot,\cdot\rangle_1$ and $\langle\cdot,\cdot\rangle_0$ is given by

$$K^* g = \partial_y T_0(x, a), \tag{3.68}$$

where T_0 is the solution to problem (1.5) with $\zeta = 0$ on Γ_1.

Proof Using the general solution (2.21), we obtain

$$T_0(x, y) = \sum_{j=1}^{\infty} \lambda_j^{1/4} M_j \frac{\sinh \sqrt{\lambda_j}(a-y)}{\sinh \sqrt{\lambda_j} a} \psi_j(x), \tag{3.69}$$

where $N_j = 0$ at $y = a$. Differentiating (3.69) with respect to y at $y = 0$, we obtain solution for $g(x)$ as follows

$$\partial_y T_0(x, 0) = -\sum_{j=1}^{\infty} \lambda_j^{3/4} M_j \frac{\cosh \sqrt{\lambda_j} a}{\sinh \sqrt{\lambda_j} a} \psi_j(x). \tag{3.70}$$

Let

$$g(x) = \sum_{j=1}^{\infty} g_j \psi_j(x), \tag{3.71}$$

Equating (3.70) in (3.71) we have

$$g_j = -\lambda_j^{3/4} M_j \frac{\cosh \sqrt{\lambda_j} a}{\sinh \sqrt{\lambda_j} a}. \tag{3.72}$$

We evaluate the coefficient M_j to get

$$M_j = -\lambda_j^{-3/4} g_j \frac{\sinh \sqrt{\lambda_j} a}{\cosh \sqrt{\lambda_j} a}. \tag{3.73}$$

Substituting (3.73) in (3.69), we get

$$T_0(x, y) = -\sum_{j=1}^{\infty} \lambda_j^{-1/2} g_j \frac{\sinh \sqrt{\lambda_j}(a-y)}{\cosh \sqrt{\lambda_j} a} \psi_j(x). \tag{3.74}$$

Differentiating (3.74) with respect to y at $y = a$ we obtain

$$K^* g = \sum_{j=1}^{\infty} g_j \frac{1}{\cosh \sqrt{\lambda_j} a} \psi_j(x). \tag{3.75}$$

By applying Lemma 2.5 and (3.60), we evaluate the inner product

$$\begin{aligned} \langle K\eta, g\rangle_0 = \gamma(T_1, T_1) &= \sum_{j=1}^{\infty} \lambda_j^{-1/2} (K\eta)_j g_j \frac{\sinh \sqrt{\lambda_j} a}{\cosh \sqrt{\lambda_j} a}, \\ &= \sum_{j=1}^{\infty} \lambda_j^{-1/2} \eta_j g_j \frac{\sinh \sqrt{\lambda_j} a}{\cosh^2 \sqrt{\lambda_j} a}, \end{aligned} \tag{3.76}$$

where $T_1 \in V(\Omega)$ solves problem (1.5). Similarly, applying Lemma 2.5 and (3.75) we compute the inner product

$$\begin{aligned}\langle \eta, K^* g\rangle_1 &= \gamma(T_0, T_0) = \sum_{j=1}^{\infty} \lambda_j^{-1/2} \eta_j (K^* g)_j \frac{\sinh \sqrt{\lambda_j} a}{\cosh \sqrt{\lambda_j} a}, \\ &= \sum_{j=1}^{\infty} \lambda_j^{-1/2} \eta_j g_j \frac{\sinh \sqrt{\lambda_j} a}{\cosh^2 \sqrt{\lambda_j} a}, \end{aligned} \tag{3.77}$$

where $T_0 \in V(\Omega)$ solves problem (1.4). Clearly from (3.76) and (3.77) we can see that

$$\langle K\eta, g\rangle_0 = \langle \eta, K^* g\rangle_1.$$

□

Let us now state and proof a lemma for compactness of the operator K and also, compute its norm.

Lemma 3.4 *The operator K defined in Definition 3.1 is compact and its norm in the spaces $H^{-1/2}(\Gamma_1)$, $H^{-1/2}(\Gamma_0)$ with the inner products $\langle\cdot,\cdot\rangle_1$ and $\langle\cdot,\cdot\rangle_0$ is equal to* $(\cosh \sqrt{\lambda_1} a)^{-1}$.

Proof From (3.60) and (3.75), we have

$$K^* K\eta = \sum_{j=1}^{\infty} (K\eta)_j \frac{1}{\cosh \sqrt{\lambda_j} a} \psi_j(x) = \sum_{j=1}^{\infty} \eta_j \frac{1}{\cosh^2 \sqrt{\lambda_j} a} \psi_j(x). \tag{3.78}$$

Hence

$$S_j^2 = \frac{1}{\cosh^2 \sqrt{\lambda_j} a}.$$

Therefore,

$$S_j \to 0 \quad \text{as} \quad j \to \infty.$$

This implies that the operator K is compact. Also, applying Lemma 2.5 and (3.60) we calculate the norm

$$\begin{aligned}\|K\eta\|_{0,\gamma}^2 &= \langle K\eta, K\eta\rangle_0 = \sum_{j=1}^{\infty} \lambda_j^{-1/2} (K\eta)_j (K\eta)_j \frac{\sinh \sqrt{\lambda_j} a}{\cosh \sqrt{\lambda_j} a}, \\ &= \sum_{j=1}^{\infty} \lambda_j^{-1/2} \eta_j^2 \frac{\sinh \sqrt{\lambda_j} a}{\cosh^3 \sqrt{\lambda_j} a}, \le \max_j \left(\frac{1}{\cosh^2 \sqrt{\lambda_j} a}\right) \sum_{j=1}^{\infty} \lambda_j^{-1/2} \eta_j^2 \frac{\sinh \sqrt{\lambda_j} a}{\cosh \sqrt{\lambda_j} a}, \\ &\le \max_j \left(\frac{1}{\cosh^2 \sqrt{\lambda_j} a}\right) \|\eta\|_{1,\gamma}^2, \le \left(\frac{1}{\cosh^2 \sqrt{\lambda_1} a}\right) \|\eta\|_{1,\gamma}^2. \end{aligned}$$

This assertions proves the lemma. □

3.1 Landweber iterative method

We now define the iterative method for solving the problem

$$K\eta = \xi, \tag{3.79}$$

where $\xi = g - \partial_y T_{(f,0)}(x,0)$ as defined in (3.61). We introduce Landweber iterative method for solving the ill-posed problem (3.79). Let $\eta_0 = 0$ be the initial approximation, compute

$$\eta_{m+1} = \eta_m + \alpha K^*(\xi - K\eta_m) = (I - \alpha K^* K)\eta_m + \alpha K^* \xi, \tag{3.80}$$

for $m = 0, 1, 2, \ldots$, where α is the relaxation parameter. It is well known that the iteration (3.80) is convergent provided that

$$0 < \alpha < \frac{2}{||K||^2}. \tag{3.81}$$

The proof is similar to that for the Richardson iteration in [36, Example 4.1]. By Lemma 3.4 this inequality can be written as

$$0 < \alpha < 2\cosh^2 \sqrt{\lambda_1} a.$$

Similarly, the iterations (3.80) converges if we have exact right hand-side in (3.79), see [18, Theorem 6.1]. As was shown in [5], the Landweber iterative method with $\alpha = 2/||K||^2$ is equivalent to the Alternating iterative method. This explains the slow convergence.

As the stopping rule for the Landweber iterations we use the Discrepancy principle [18]. The Discrepancy principle is applied as follows: Let $\xi \in H^{-1/2}(\Gamma_0)$ be the exact data and $\xi^\delta \in H^{-1/2}(\Gamma_0)$ be an approximation of ξ satisfying

$$\|\xi - \xi^\delta\|_{H^{-1/2}(\Gamma_0)} \leq \delta. \tag{3.82}$$

Consider the Landweber iterations

$$\eta_{m+1}^\delta = \eta_m^\delta + \alpha K^*(\xi - K\eta_m^\delta) = (I - \alpha K^* K)\eta_m^\delta + \alpha K^* \xi, \quad m = 0, 1, \ldots \tag{3.83}$$

where $0 < \alpha < 2\cosh^2 \sqrt{\lambda_1} a$. Let $\tau > 1$. The iterations are terminated when

$$\|\xi^\delta - K\eta_m^\delta\|_{H^{-1/2}(\Gamma_0)} \leq \tau\delta. \tag{3.84}$$

The stopping index is denoted by

$$m = m(\delta, \xi^\delta).$$

Note that $m(\delta, \xi^\delta) \to \infty$ as $\delta \to 0$. Thus the following theorem [25, Theorem 2.15 and Theorem 2.19] guarantees convergence.

Theorem 3.5 *Let $\xi,\ \xi^\delta \in H^{-1/2}(\Gamma_0)$, and $\|\xi - \xi^\delta\|_{H^{-1/2}(\Gamma_0)} \leq \delta$. Then the Landweber iterations, together with the Discrepancy principle, satisfies*

$$\eta_{m(\delta,\xi^\delta)}^\delta \to \eta \quad as \quad \delta \to 0.$$

Note that for the discrepancy principle in (3.84) the residual norm, i.e. the left side can be computed in each iteration. For the numerical experiments we know the exact data ξ. Thus, we can compute δ by evaluating the norm in (3.82). For practical application the exact data is unknown. Since we assume normally distributed random noise it is more natural to assume a bound of (3.82) in the L^2 norm. However, the point of the experiment section is to illustrate the theoretical part of the paper. Thus, we use the norms in $H^{-1/2}$. Note however that the L^2 norm is stronger than $H^{-1/2}$ norms. Thus we could implement the discrepancy principle (3.84) using L^2 norm instead.

4 Numerical results

In this section, we present numerical experiments for the Landweber iterative method analysed in the previous section. To conduct the experiments, we implement a finite difference method for solving the two auxiliary problems (1.4) and (1.5). Let a and b be positive numbers and recall that the domain is given as

$$\Omega = (0, b) \times (0, a), \quad \text{with } \Gamma_0 = (0, b) \times \{0\} \text{ and } \quad \Gamma_1 = (0, b) \times \{a\}.$$

To carry out the tests, we consider the following Cauchy problem for stationary heat equation in Ω, i.e.

$$\begin{cases} -\frac{\partial}{\partial x}\left(c(x)\frac{\partial T}{\partial x}\right) - \frac{\partial}{\partial y}\left(c(x)\frac{\partial T}{\partial y}\right) + \frac{2h}{k}\sqrt{1+(c'(x))^2}T = 0, & 0 < x < b, 0 < y < a, \\ T_y(x, 0) = g(x), & 0 \le x \le b, \\ T(x, 0) = f(x), & 0 \le x \le b, \\ \lim_{x\to 0,b} c(x)T_x(x, y) = 0 & 0 \le y \le a. \end{cases} \tag{4.85}$$

To compute the numerical solutions, we discretize the differential equation in (4.85) on a uniform grid of size $N \times M$. Since the grid is uniform the number of grid points M in the $y-$ directions is uniquely determined by N. We consider a standard accuracy of $\mathcal{O}(dx^2)$ in the finite difference approximation. Let $T_{i,j}$ be the discrete approximation to $T(x_i, y_j)$. The finite difference approximation for the equation on each interior grid points (x_i, y_j) is given by

$$-c_{i+1/2}T_{i+1,j} - c_{i-1/2}T_{i-1,j} + dT_{i,j} - c_i\left(T_{i,j+1} + T_{i,j-1}\right) = 0,$$

where

$$d = \left(c_{i+1/2} + c_{i-1/2} + 2c_i + \frac{2h}{k}(dx)^2\sqrt{1+(c_i')^2}\right).$$

We cannot implement the degenerate boundary condition,

$$\lim_{x\to 0,b} c(x)T_x(x, y) = 0, \tag{4.86}$$

directly, since $c(x)$ tends to zero near the boundary. This means that we can get unbounded solutions. An alternative boundary condition that allows for similar solutions is considered. We choose the second order derivative

$$(T_{1,j} - 2T_{2,j} + T_{3,j})(dx)^{-2} = 0, \qquad j = 2, \ldots, M-1,$$

with a standard accuracy of $\mathcal{O}(dx^2)$. The boundary $i = N$ is treated similarly. This allows for functions that behave like a straight line near the boundary. This type of solution also satisfies the original boundary conditions (4.86).

Similarly, for the boundaries corresponding to $y = 0$, and $y = a$ one can obtain different equations by taking into the consideration the boundary condition given. For the case of Dirichlet boundary conditions, we obtain the discretization as follows:

$$T_{i,j} = d_i^j, \qquad i = 1, \ldots N, \quad j = 1 \quad \text{or} \quad j = M,$$

where d_i^j is the Dirichlet data given at $y = 0$ or $y = a$. Furthermore, the discretization of the Neumann boundary conditions is given by

$$(-3T_{i,1} + 4T_{i,2} - T_{i,3})(2dx)^{-1} = n_i^j, \qquad i = 1, \ldots N,$$

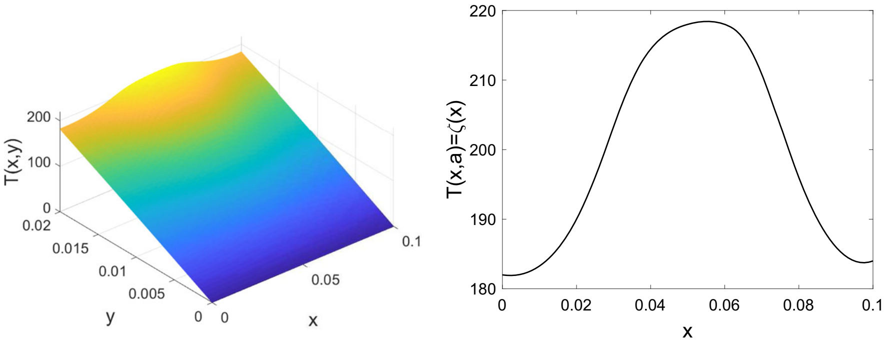

Fig. 3 Numerical solution $T(x, y)$ (left), and the Dirichlet data $T(x, a) = \zeta(x)$ (right)

n_i^j is the given Neumann data at $y = 0$ with a standard accuracy of $\mathcal{O}(dx^2)$. The case $y = a$ is similar. For further detail about the boundary conditions one can refer to [9].

To create a test problem which is suitable for our problem, we choose $a = 0.02$ and $b = 0.1$ with a grid size $N = 501$ which gives $M = 101$. The same grid is used in all our experiments. Similarly, we chose also

$$c(x) = \frac{b}{10} \sin(\pi x/b),$$

$k = 3$, and $h = 0.25$ respectively. The same values also are used in all the computations. We used cubic spline interpolation to create the Dirichlet data $\zeta(x)$, $\quad 0 \leq x \leq b$. We then solved the differential equation in (4.85), with boundary conditions $T(x, a) = \zeta(x)$, and $T(x, 0) = 0$. From Definition 3.1 of the operator, we see that $f(x) = 0$. By solving this problem, we create a numerical test problem. The numerical solution $T(x, y)$, and the Dirichlet data $\zeta(x)$ are illustrated in Fig. 3. Using the numerical solution $T(x, y)$, we compute the Neumann data at Γ_0, and Γ_1 respectively, i.e. we obtain the exact data η on Γ_1 and ξ on Γ_0 that satisfy $K\eta = \xi$.

Recall that both η and ξ are vectors, i.e.

$$\xi := (\xi_j) \qquad j = 1, \ldots, m,$$

and

$$\eta := (\eta_j) \qquad j = 1, \ldots, m,$$

In the case where noise is present, we add normally distributed random noise of variance β to the exact data ξ to obtain

$$\xi^\delta = \xi + \beta * randn(size(\xi)), \tag{4.87}$$

i.e.

$$\xi_j^\delta = \xi_j + \beta_j, \qquad j = 1, \ldots, m.$$

Example 4.1 In our first test example, we compute the solution of $K\eta^\delta = \xi^\delta$ using the Landweber iteration and also the Dirichlet–Neumann alternating algorithm. We use the parameter value $\alpha = 1.0$, and noise free data, i.e. noise level $\beta = 0$. We choose the initial guess $\eta_0 = \zeta_0 = 0$, and we compute the approximate solutions η_m and ζ_m. The numerical solutions obtained are of very good quality. We can see that both the errors $\|\eta_m - \eta\|_{\gamma,\Gamma_1}$,

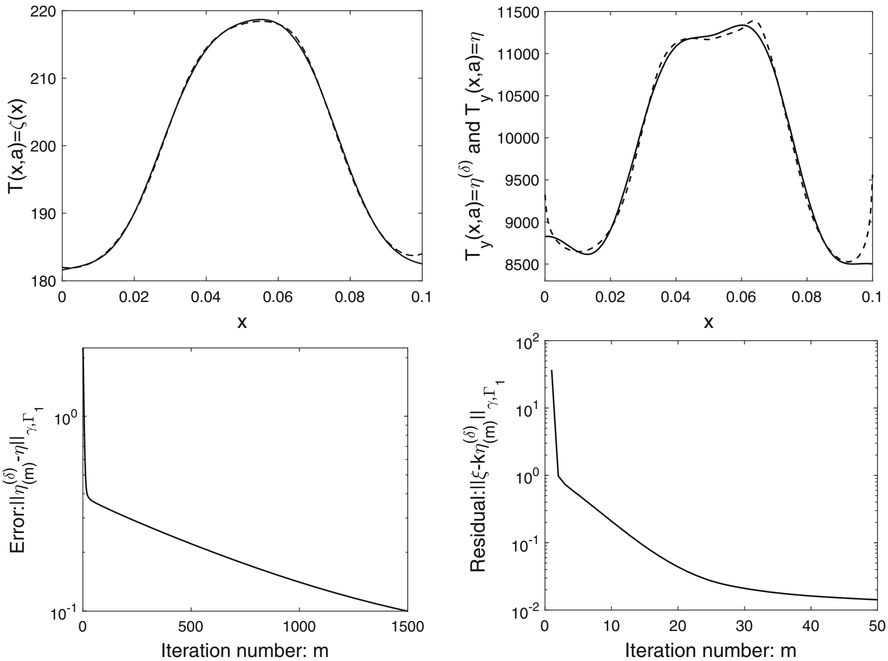

Fig. 4 We display the approximate solution $T_\alpha^{(1500)}(x, a)$ using the Landweber iteration and the Dirichlet–Neumann alternating algorithm with $\alpha = 1.0$ (top, left black curve), and the exact solution (top, left black dashed curve) using noise level $\beta = 0$. Similarly, we display the approximate Neumann data $T_y^{(1500)}(x, a)$ (top, right black curve), and exact Neumann data η (top, right black dashed curve). We also display the errors (bottom, left curve) $||\eta_m^\delta - \eta||_{\gamma,\Gamma_1}$, and the residuals (bottom, right curve) $||\xi^\delta - K\eta_m^\delta||_{\gamma,\Gamma_0}$. The graphs for both methods are identical

and residuals $||\xi - K\eta_m||_{\gamma,\Gamma_0}$ are monotonically decreasing. We also observe that the rate of convergence is quite slow. The graphs for both methods are identical. The results are displayed in Fig. 4.

Example 4.2 In our second test example, we solve $K\eta^\delta = \xi^\delta$ using the Landweber iteration. The parameter value chosen are $\alpha = 1.0$, the noise levels are $\beta = 4 \cdot 10^1$ and $12 \cdot 10^1$, and $\tau = 1.1$. The exact data and noisy data are displayed in Fig. 5. We see that the noise level is quite significant in both cases.

For the noise level $\beta = 4 \cdot 10^1$, we have seen that the solution obtained is of good quality. This shows that acceptable solutions can be found with realistic noise levels. We also displayed the errors $||\eta_m^\delta - \eta||_{\gamma,\Gamma_1}$, and residuals $||\xi^\delta - K\eta_m^\delta||_{\gamma,\Gamma_0}$. We have observed that minimum norm solution and the smallest total error is reached after 871 iterations. Similarly, the residual is monotonically decreasing, and the discrepancy principle is achieved after 41 iterations. The results are displayed in Fig. 6. In the case of the noise level $\beta = 12 \cdot 10^1$, we can see that the solution obtained is also of good quality. We also presented the errors $||\eta_m^\delta - \eta||_{\gamma,\Gamma_1}$, and residuals $||\xi^\delta - K\eta_m^\delta||_{\gamma,\Gamma_0}$. We have found out that the smallest total error is achieved after 474 iterations. The residual curve is also monotonically decreasing, and the discrepancy principle is satisfied after 21 iterations. The numerical results are displayed in Fig. 7. In both cases, we see that the errors decrease up-to a certain number of iterations and then it starts to increase. This is known as semi-convergences effect. From the residuals

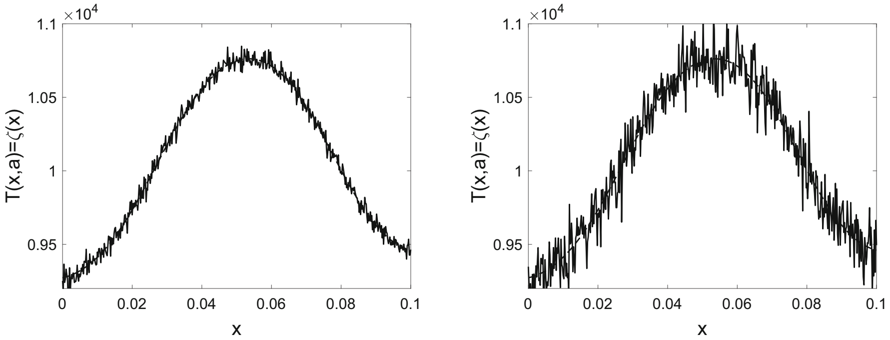

Fig. 5 We display both the exact data ξ (black dashed curve) and the noisy data ξ^{δ} (black curve). On the left, we used noise levels $\beta = 4 \cdot 10^{1}$ and $\beta = 12 \cdot 10^{1}$ on the right

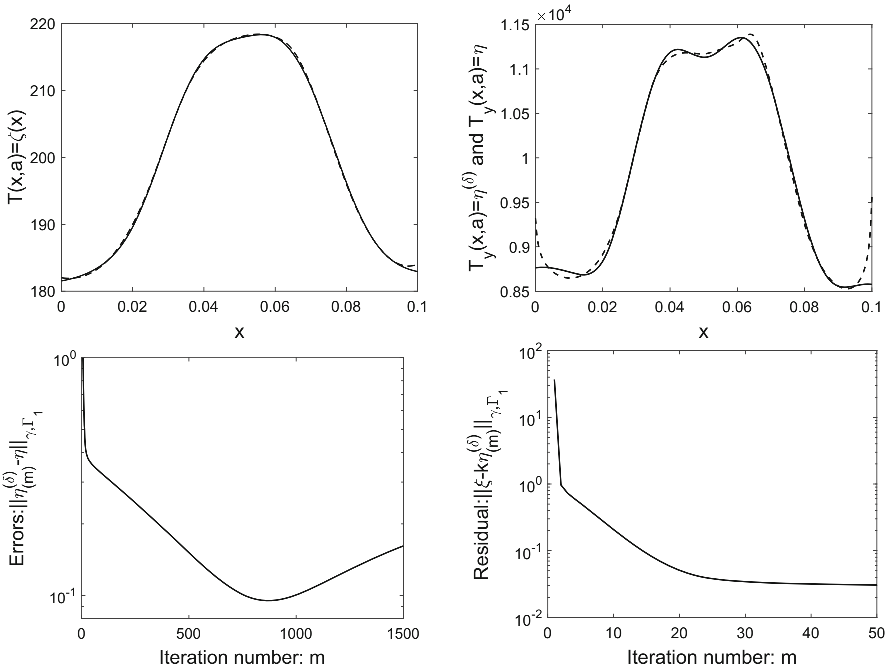

Fig. 6 We display the approximate solution $T_{\alpha}^{(871)}(x, a)$ using the noise level $\beta = 4 \cdot 10^{1}$ (top, left black curve) and Neumann boundary data $T_{y}^{(871)}(x, a)$ (top, black right curves). We also displayed the exact data (black, dashed curves) in both graphs. We present also the convergence for errors $||\eta_{m}^{\delta} - \eta||_{\gamma,\Gamma_1}$ (bottom, left curve), and residuals $||\xi^{\delta} - K\eta_{m}^{\delta}||_{\gamma,\Gamma_0}$ (bottom, right curve). Here, the value of $\tau = 1.1$ is used

curves, we noted that the discrepancy principle is underestimating the optimal iterations numbers.

Example 4.3 In our last test example, we investigate the effect of relaxation parameter α in the Landweber iterations by solving $K\eta^{\delta} = \xi^{\delta}$. The parameter values used are $\alpha = 1.9, 2.0,$

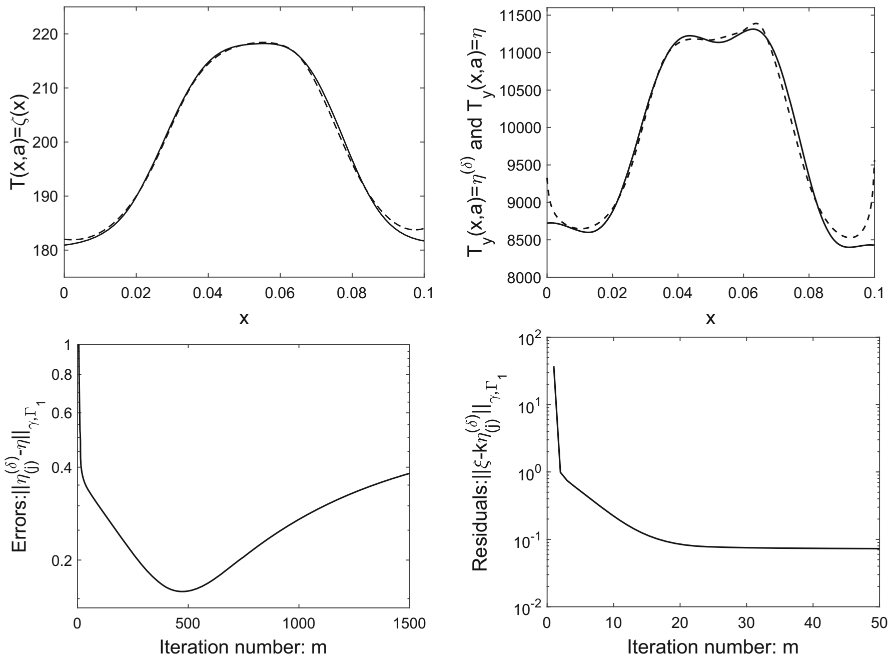

Fig. 7 We display the approximate solution $T_{\alpha}^{(474)}(x, a)$ using the noise level $\beta = 12 \cdot 10^1$ (top, left black curve). Also, we show the exact solution (black dashed curve). Similarly, we display the approximate Neumann data $T_y^{(474)}(x, a)$(top, right black curve). The exact Neumann data η (black dashed curve) is also displayed. Finally, the convergence for errors $||\eta_m^{\delta} - \eta||_{\gamma,\Gamma_1}$ (bottom, left curve), and residuals $||\xi^{\delta} - K\eta_m^{\delta}||_{\gamma,\Gamma_0}$ (bottom, right curve) is display. We have used also $\tau = 1.1$

and 2.1, and the noise level $\beta = 4 \cdot 10^1$. In Fig. 8, we displayed the errors $||\eta_m^{\delta} - \eta||_{\gamma,\Gamma_1}$, and residuals $||\xi^{\delta} - K\eta_m^{\delta}||_{\gamma,\Gamma_0}$.

The results indicates that the Landweber iteration converges for $\alpha \lesssim 2$. We also observed that the rate of converges is faster for smaller values of α as compare to larger one. If we compare with the theoretical result (3.81) we have an indication that the norm of the operator K is equal to 1. By looking at Lemma 3.4 this allows us to compute λ_1.

5 Conclusions

In this paper, we consider steady state heat conduction in a thin plate. The thin plate connects two cylindrical containers. Its purpose is to fix their relative positions and at the same time to measure the temperature on the inner cylinder. We derive a two dimensional mathematical model, and use it to approximate the heat conduction in the thin plate. Since the plate has sharp edges on the sides, the resulting equation we obtained is a degenerate elliptic equation. The application of the Alternating iterative algorithm for solving a degenerate elliptic equation is new for this study.

To find the temperature on the interior part from the exterior measurements, we formulate the problem as a Cauchy problem for stationary heat equation. Furthermore, we describe two boundary value problems (1.4) and (1.5), and showed that they are well-posed. Similarly, we

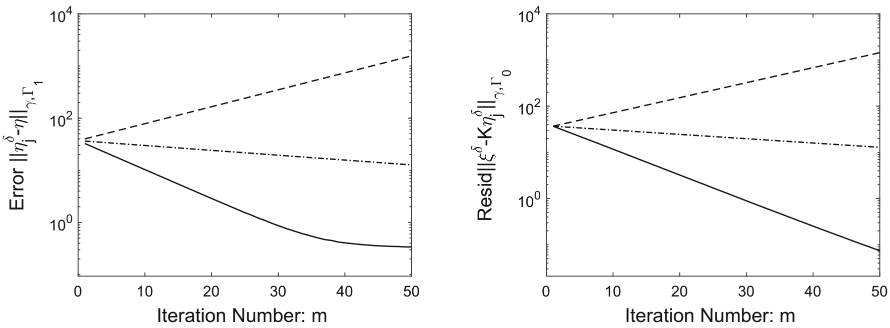

Fig. 8 We display the errors $||\eta_m^\delta - \eta||_{\gamma,\Gamma_1}$ (left curves), and the residual $||\xi^\delta - K\eta_m^\delta||_{\gamma,\Gamma_0}$ (right curves) using noise level $\beta = 4 \cdot 10^1$. We have used here $\alpha = 1.9$ (black curve), $\alpha = 2.0$ (dashdot curve) and $\alpha = 2.1$ (dashed curve)

analysed the convergence of the Dirichlet–Neumann alternating algorithm for solving the Cauchy problem (1.3). Moreover, we have reformulated the Cauchy problem as an operator equation, with a compact operator, and applied the Landweber iteration method to solve the problem. We have shown that the Discrepancy principle works for this case and we have a regularization method.

From our numerical experiments, we see that it is possible to obtained good quality solutions, even in the presence of large noise. We also see that in all cases the residual norms are monotonically decreasing. This means that the Discrepancy principle can be applied in practice. We also compute errors during the Landweber iterations. The results seem to indicate that the Discrepancy principle underestimate the optimal number of iterations. We also see the semi-convergence effect in the error curves. From the numerical computation, we have seen that ill-posedness depends strongly on the geometry of the domain [7]. Hence for this application to work the inner and outer cylinder has to be relatively close.

In future work, instead of Dirichlet–Neumann Alternating algorithm and the corresponding operator equation, we will consider using Dirichlet–Robin boundary conditions in the alternating algorithm. We will also consider methods with faster convergences rates such as the Conjugate gradient method. In order to implement the Conjugate gradient method we need to reformulate the alternating algorithm as a Landweber iteration for a specific operator equation. In this context, for this to work, we need to develop the scalar product that allows for the computation of the adjoint operator and also appropriate norms. With the adjoint operator in place we can implement the Conjugate gradient method. To improve on the stability of the solutions we will consider using Tikhonov regularization method.

Funding Open access funding provided by Linköping University.

Data availability We have no measured data in this article and so there is nothing that we needs to be made public.

Declarations

Conflict of interest There is no conflict of interest.

References

1. Achieng, P., Berntsson, F., Chepkorir, J., Kozlov, V.A.: Analysis of Dirichlet–Robin iterations for solving the Cauchy problem for elliptic equations. Bull. Iran. Math. Soc. **47**(6), 1681–1699 (2021)
2. Bastay, G., Johansson, T., Kozlov, A.V., Lesnic, D.: An alternating method for the stationary Stokes system. ZAMM Z. Angew. Math. Mech. **86**(4), 268–280 (2006)
3. Berntsson, F.: Sequential solution of the sideways heat equation by windowing of the data. Inverse Probl. Eng. **11**(2), 91–103 (2003)
4. Berntsson, F.: An inverse heat conduction problem and improving shielded thermocouple accuracy. Numer. Heat Transfer Part A Appl. **61**(10), 754–763 (2012)
5. Berntsson, F., Chepkorir, J., Kozlov, V.A.: Accelerated Dirichlet–Robin alternating algorithms for solving the Cauchy problem for the Helmholtz equation. IMA J. Appl. Math. **86**(6), 1181–1203 (2021)
6. Berntsson, F., Eldén, L.: Numerical solution of a Cauchy problem for the Laplace equation. Inverse Probl. **17**(4), 839–853 (2001)
7. Berntsson, F., Kozlov, V.A., Mpinganzima, L., Turesson, B.: Numerical Solution of the Cauchy Problem for the Helmholtz Equation. Linköping University Electronic Press, Linköping (2014)
8. Berntsson, F., Kozlov, V.A., Mpinganzima, L., Turesson, B.O.: An accelerated alternating procedure for the Cauchy problem for the Helmholtz equation. Comput. Math. Appl. **68**(1–2), 44–60 (2014)
9. Berntsson, F., Kozlov, V.A., Mpinganzima, L., Turesson, B.O.: An alternating iterative procedure for the Cauchy problem for the Helmholtz equation. Inverse Probl. Sci. Eng. **22**(1), 45–62 (2014)
10. Berntsson, F., Kozlov, V.A., Mpinganzima, L., Turesson, B.O.: Iterative Tikhonov regularization for the Cauchy problem for the Helmholtz equation. Comput. Math. Appl. **73**(1), 163–172 (2017)
11. Carasso, A.: Determining surface temperatures from interior observations. SIAM J. Appl. Math. **42**(3), 558–574 (1982)
12. Chapko, R., Johansson, B.T.: An alternating potential-based approach to the Cauchy problem for the Laplace equation in a planar domain with a cut. Comput. Methods Appl. Math. **8**(4), 315–335 (2008)
13. Deng, Y., Liu, Z.: Iteration methods on sideways parabolic equations. Inverse Probl. **25**(9) (2009)
14. Eldén, L.: Approximations for a Cauchy problem for the heat equation. Inverse Probl. **3**(2), 263–273 (1987)
15. Eldén, L.: Numerical solution of the sideways heat equation by difference approximation in time. Inverse Probl. **11**(4), 913–923 (1995)
16. Eldén, L., Berntsson, F., Regińska, T.: Wavelet and Fourier methods for solving the sideways heat equation. SIAM J. Sci. Comput. **21**(6), 2187–2205 (2000)
17. Eldén, L., Simoncini, V.: A numerical solution of a Cauchy problem for an elliptic equation by Krylov subspaces. Inverse Probl. **25**(6), 065002 (2009)
18. Engl, H., Hanke, M., Neubauer, A.: Regularization of Inverse Problems, vol. 375. Kluwer Academic Publishers Group, Dordrecht (1996)
19. Golriz, M.R., Sundén, B.: A method for temperature measurements in circulating fluidized bed combustors. Exp. Therm. Fluid Sci. **9**(3), 274–282 (1994)
20. Hadamard, J.: Lectures on Cauchy's Problem in Linear Partial Differential Equations. Dover Publications, New York (1953)
21. Hào, D.N., Reinhardt, H.J., Schneider, A.: Numerical solution to a sideways parabolic equation. Int. J. Numer. Methods Eng. **50**(5), 1253–1267 (2001)
22. Holman, J.P.: Heat Transfer, 10th edn. McGraw Hill, New York (2010)
23. Jahedi, M., Berntsson, F., Wren, J., Moshfegh, B.: Transient inverse heat conduction problem of quenching a hollow cylinder by one row of water jets. Int. J. Heat Mass Transfer **117**, 748–756 (2018)
24. Johansson, B.T., Kozlov, V.A.: An alternating method for Cauchy problems for Helmholtz-type operators in non-homogeneous medium. IMA J. Appl. Math. **74**(1), 62–73 (2009)
25. Kirsch, A.: An Introduction to the Mathematical Theory of Inverse Problems, vol. 120. Springer Science and Business Media, New York (2011)
26. Kozlov, V.A., Maz'ya, V.G.: Iterative procedures for solving ill-posed boundary value problems that preserve the differential equations. Algebra i Analiz **1**(5), 1207–1228 (1989)

27. Kozlov, V.A., Maz'ya, V.G., Fomin, A.V.: An iterative method for solving the Cauchy problem for elliptic equations. Comput. Math. Math. Phys. **31**(1), 62–73 (1991)
28. Landweber, L.: An iteration formula for Fredholm integral equations of the first kind. Amer. J. Math. **73**(3), 615–624 (1951)
29. Lesnic, D., Elliott, L., Ingham, D.B.: Application of the boundary element method to inverse heat conduction problems. Int. J. Heat Mass Transfer **39**(7), 1503–1517 (1996)
30. Lesnic, D., Elliott, L., Ingham, D.B.: An alternating boundary element method for solving Cauchy problems for the biharmonic equation. Inverse Probl. Eng. **5**(2), 145–168 (1997)
31. Marin, L.: Landweber–Fridman algorithms for the Cauchy problem in steady-state anisotropic heat conduction. Math. Mech. Solids **25**(6), 1340–1363 (2020)
32. Maxwell, D.: Kozlov–Maz'ya iteration as a form of Landweber iteration. Inverse Probl. Imaging **8**(2), 537–560 (2014)
33. McLean, W.: Strongly Elliptic Systems and Boundary Integral Equations. Cambridge University Press, Cambridge (2000)
34. Ngendahayo, J.P., Niyobuhungiro, J., Berntsson, F.: Estimation of surface temperatures from interior measurements using Tikhonov regularization. Results Appl. Math. **9** (2021)
35. Prud'Homme, M., Nguyen, T.H.: Fourier analysis of conjugate gradient method applied to inverse heat conduction problems. Int. J. Heat Mass Transfer **42**(24), 4447–4460 (1999)
36. Saad, Y.: Iterative Methods for Sparse Linear Systems. SIAM, Philadelphia (2003)
37. Voinea, M., Andreea, P., Marin, L.: Fading regularization MFS algorithm for the Cauchy problem in anisotropic heat conduction. Comput. Mech. **68**(4), 921–941 (2021)
38. Wikström, P., Blasiak, W., Berntsson, F.: Estimation of the transient surface temperature, heat flux and effective heat transfer coefficient of a slab in an industrial reheating furnace by using an inverse method. Steel Res. Int. **78**(1), 63–70 (2007)
39. Xiong, X.T., Fu, C.L.: A spectral regularization method for solving surface heat flux on a general sideways parabolic. Appl. Math. Comput. **197**(1), 358–365 (2008)
40. Yu-Ching, Y., Chen, W.: A nonlinear inverse problem in estimating the heat flux of the disc in a disc brake system. Appl. Therm. Eng. **31**(14–15), 2439–2448 (2011)